Chinese Journal of
POLYMER SCIENCE

RESEARCH ARTICLE

https://doi.org/10.1007/s10118-025-3413-8
Chinese J. Polym. Sci. **2025**, *43*, 2030–2041

Amine-reactive Polymer Platform for Engineering Surface Modification of Next-generation Sequencing Chips

Wei Tian[a], Xin-Yuan Wang[a], Die-Wen Feng[b], Xiang-Qian Li[a], Yue-Kang Jin[c*], Hui Li[a*], and Hao Liu[a*]

[a] *State Key Laboratory of Advanced Fiber Materials, Center for Advanced Low-Dimension Materials, Donghua University, Shanghai 201620, China*
[b] *Salus BioMed Company, Shenzhen 518106, China*
[c] *Institute of Advanced Technology, University of Science and Technology of China, Hefei 230026, China*

Electronic Supplementary Information

Abstract In this study, an amine-reactive poly(pentafluorophenyl acrylate) (**PPFPA**) platform was developed for advanced surface engineering of next-generation sequencing (NGS) chips. Through post-polymerization modification, **PPFPA** was functionalized with dual moieties: azide groups for covalent immobilization of DBCO-modified DNA primers *via* click chemistry and tunable hydrophilic side chains to optimize biocompatibility and surface properties. Systematic screening revealed that hydrophobic azide carriers combined with neutral hydroxyl groups maximized the DNA immobilization efficacy, approaching the performance of commercial polyacrylamide-based polymers. The negatively charged carboxyl groups severely impede DNA primer attachment. Higher molecular weight derivatives further enhance the efficacy of DNA immobilization. In NGS validation, optimized surface modification polymers achieved robust surface density of clustered DNA and high sequencing accuracy, surpassing quality benchmarks and comparable to those of conventional analogs. This platform demonstrates significant potential for tailoring high-sensitivity surfaces for genomic applications, advancing clinical diagnostics, and personalized medicine.

Keywords Next-generation sequencing; Surface modification polymers; Poly(pentafluorophenyl acrylate); DNA immobilization

Citation: Tian, W.; Wang, X. Y.; Feng, D. W.; Li, X. Q.; Jin, Y. K.; Li, H.; Liu, H. Amine-reactive polymer platform for engineering surface modification of next-generation sequencing chips. *Chinese J. Polym. Sci.* **2025**, *43*, 2030–2041.

INTRODUCTION

Gene sequencing is a cornerstone of modern biotechnology, playing a pivotal role in applications such as detecting genetic diseases in newborns,[1,2] diagnosing infectious diseases,[3,4] and guiding personalized medicine.[5,6] With the ability to provide critical insights into genetic information, gene sequencing empowers individuals and healthcare providers to make informed decisions, ultimately leading to improved health outcomes and quality of life.[7] Since the 1970s,[8] gene sequencing techniques have undergone explosive development and have become an indispensable tool in modern biological and medical research. To date, significant cost reduction [9] and substantial increase in throughput[10] have enabled large-scale genome projects and precision medicine research. In the field of clinical diagnostics, gene sequencing has become a powerful tool for early disease detection[11] and risk assessment,[12] enabling the identification of genetic predispositions to various conditions, including cancer[13] and hereditary disorders.[14]

Early developed DNA sequencing methods, such as Sanger sequencing,[7,15] have long been regarded as the "gold standard" due to their high accuracy and reliability. However, these methods are limited by their low throughput[16,17] and labor-intensive[18] processes. Next-generation sequencing (NGS) techniques have revolutionized the field by simultaneously enabling high-throughput sequencing of a large number of DNA fragments.[19,20] Despite these advancements, challenges remain in achieving sufficient detection sensitivity[21] and efficiency[22] particularly for the immobilization of DNA probes on sequencing chips.[23,24] Briefly, the main procedures of NGS techniques include fragmented gene library preparation, sequencing by synthesis (SBS),[25] and data analysis, among which bridge polymerase chain reaction (PCR)[26] during SBS is one of the most crucial steps. In bridge PCR, the surface modification polymer must be both highly reactive and selective to immobilize DNA primers on sequencing chips and possess good biocompatibility.[27–29] In current commercial NGS solutions, DNA primers decorated with dibenzocyclooctyne (DBCO) are grafted onto the surface of sequencing chips coated with azide-carrying polymers,[30,31] which must be hydrophilic, biocompatible, and compatible with bridge PCR. To fulfil these requirements, the surfaces of slides or specialized structures are often subjected to chemical treatment with silanes, polyethylene gly-

* Corresponding authors, E-mail: jinyk@mail.ustc.edu.cn (Y.K.J.)
E-mail: lihui@dhu.edu.cn (H.L.)
E-mail: liuh@dhu.edu.cn (H.L.)

Received June 10, 2025; Accepted July 9, 2025; Published online September 2, 2025

col, pluoronics, proteins, or other surface modifying agents. These surface modification[32–34] chemistries typically lack precise stoichiometric controls. In Sanger sequencing, polyacrylamide (PAAm)[35] was used in capillary electrophoresis to separate DNA fragments of varying lengths, exhibiting good biocompatibility. Consequently, when attempting to develop NGS techniques, PAAm was naturally chosen for the surface modification of sequencing chips.[36] Therefore, there is a lack of systematic research on other biocompatible hydrophilic polymers as sequencing chip surface modification agents and their performance in gene sequencing. Existing surface modification strategies for NGS chips have limitations such as complex procedures and imprecise stoichiometric control,[32–34] creating an urgent need for more efficient and adaptable solutions. Many current methods involve multiple steps and harsh conditions, which not only increase the risk of operational errors but also lead to higher production costs and longer processing time.[32] Furthermore, some methods lack sufficient customization flexibility, restricting their application across different sequencing platforms and in various scenarios.[33]

In this study, we attempted to develop a universal polymer platform,[37] poly(pentafluorophenyl acrylate) (**PPFPA**), which can effectively graft azide[38] and hydrophilic side groups[39] in a post-polymerization manner (see Fig. 1a).[40] The PPFPA platform[37] addresses these challenges by providing a simplified, efficient, and cost-effective surface modification approach. Its design allows for precise control over the stoichiometry of functional groups on the chip surface, enhancing the DNA probe immobilization efficiency and accuracy. The platform's high reactivity and selectivity ensured robust and stable surface modifications, guaranteeing consistent sequencing performance. In addition, its exceptional flexibility enables customization to meet the specific requirements of various sequencing platforms and applications. As a great merit of **PPFPA**,[41] the active pentafluorophenyl (PFP) ester[42–44] group can selectively react with amine species, which makes it possible for post-polymerization[45] treatment by the desired amine species. Here, we designed two types of azide-bearing amine species, **NH_2-C_5-N_3** and **NH_2-EG_3-N_3** (denoted as monomer **1**, see Fig. 1a), to react with a small portion of PFP active esters to immobilize the **DBCO-P7LG** and **DBCO-P5LU** primers.[46,47] Consequently, four different kinds of amine species (denoted as monomer **2**, see Fig. 1a): isopropanolamine (**IPA**), glycine (**Gly**), 3-aminopropanamide (**APA**), and ammonia solution (**AS**), were applied to consume the rest PFF ester groups, introducing versatile hydrophilic functionalities and charge states. The resulting polymers with different combinations of monomers **1** and **2** were applied to the surface modification of the NGS chips. DNA primer immobilization efficacy and gene sequencing performance were also investigated. Through systematic comparison of functional groups, molecular weight, and modification conditions on the basis of the **PPFPA** platform, we obtained optimized surface modification polymers that demonstrated superior DNA primer immobilization efficacy, preserved probe functionality, and sensitivity comparable to commercial PAAm-based copolymers. These results highlight the **PPFPA** platform's great potential of the PPFPA platform for designing and screening high-performance surface-graft polymers for more advanced NGS applications, offering significant promise for clinical diagnostics, personalized medicine, and advanced ge-

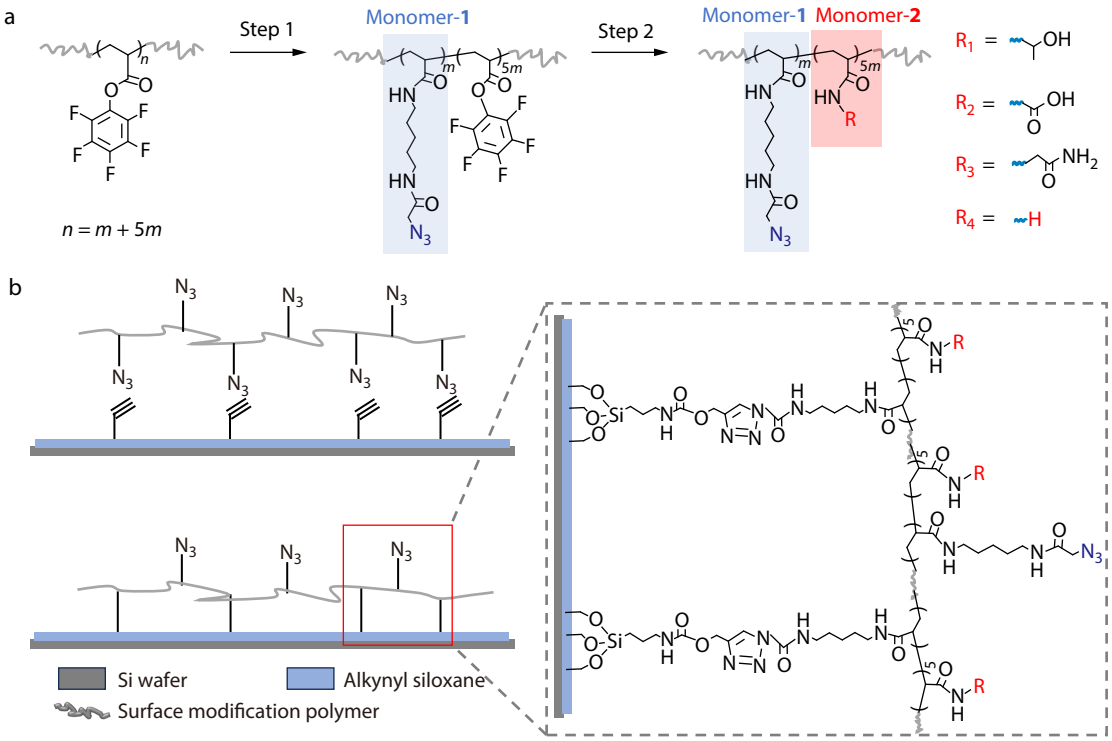

Fig. 1 Schematic diagram showing (a) the post-polymerization transformation of the **PPFPA** platform by amine species, and (b) the covalent anchoring of the surface modification polymers.

https://doi.org/10.1007/s10118-025-3413-8

nomic research. Furthermore, the versatility of the **PPFPA** platform suggests that it could be adapted for use in a wide range of detection systems and assay formats, potentially broadening the scope of genetic testing and enabling more precise and efficient genetic analyses in diverse research and clinical settings.

MATERIALS AND METHODS

Materials

2,2-Azobis(2-methylpropionitrile) (AIBN) was purchased from Sigma Aldrich. Pentafluorophenol, prop-2-yn-1-yl(3-(triethoxysilyl)propyl)carbamate, *N*-(3-dimethylaminopropyl)-*N*'-ethylcarbodiimide hydrochloride (EDC·HCl), ethyl azidacetate, tert-butyl (5-aminopentyl)carbamate, were purchased from Bide Pharmatech Co., Ltd. 3× Saline sodium citrate buffer (SSC) were purchased from Beyotime Co., Ltd. Acrylic acid and 2-azidoacetic acid were purchased from Aladdin Biochemical Technology Co. Ltd. Dichloromethane (DCM), petroleum ether (PE), ethyl acetate (EA), diethyl ether, 1,4-dioxane, tetrahydrofuran (THF), methanol, ethanol, isopropanol, hydrochloric acid (HCl), 1-hydroxybenzotriazole (HOBt), triethylamine (TEA), isopropanol (**IPA**), glycine (**Gly**), 3-aminopropanamide (**APA**), ammonia solution (**AS**), and *N*,*N*-diisopropylethylamine (DIPEA) were purchased from Shanghai Titan Scientific Co., Ltd.

Synthesis of PFPA

In a round-bottom flask equipped with a magnetic stirrer, 7.11 g (98.0 mmol) of acrylic acid and 20.0 g (108 mmol) of pentafluorophenol were dissolved in 140 mL of DCM. 22.7 g (119 mmol) of EDC·HCl dissolved in 140 mL of DCM was added dropwise to the flask. The reaction was performed for 12 h with vigorous stirring at room temperature. The product was washed 3 times with saturated saltwater and dried over $MgSO_4$. After removing the solvent, the product was purified by column chromatography using petroleum ether (PE). The product was isolated by solvent evaporation and further dried in a vacuum oven at room temperature to yield a light brown liquid. Yield 17.0 g (72.0%).

Synthesis of PPFPA

PFPA and AIBN were added in a Schlenk flask at a certain ratio. Then, 2.00 mL of 1,4-dioxane was added to the flask. The flask was then purged with nitrogen for 30 min to remove oxygen. The flask was sealed and placed in an oil bath at 70 °C for 24 h. The product was precipitated twice using cold methanol. Finally, the resulting white product was dried overnight in a vacuum oven.

Synthesis of *N*-(5-aminopentyl)-2-azidoacetamide (NH_2-C_5-N_3)

428 mg (4.23 mmol) of 2-azidoacetic acid and 714 mg (3.53 mmol) of tert-butyl (5-aminopentyl) carbamate (714 mg, 3 mmol) were added to a round-bottom flask, followed by addition of 10 mL of dichloromethane. Subsequently, 572 mg (4.23 mmol) of HOBt and EDC·HCl (812 mg (4.23 mmol) were added to the mixture. The reaction was carried out overnight in an ice-water bath at 0 °C. After completion of the reaction, the mixture was washed with saturated brine. The solvent was removed by rotary evaporation, and the tert-butyl (5-(2-azidoacetamido) pentyl) carbamate residue was dried in a vacuum oven overnight. An appropriate amount of dried sample was added to an ethyl acetate solution of HCl. The mixture was then stirred overnight at room temperature. After the reaction, the solution was concentrated *via* rotary evaporation to obtain **NH_2-C_5-N_3** as a white solid, which was then dried overnight in a vacuum oven.

Synthesis of P(N_3-PFPA)

250 mg of **PPFPA** was added into small glass vials and dissolved using 50.0 mL of THF. Subsequently, 38.8 mg (0.0170 mmol) **NH_2-C_5-N_3** was added, followed by the addition of 100 μL TEA. The reaction proceeded for 2 h at room temperature. The product was precipitated, washed twice in cold methanol, and filtered for collection. Finally, it was dried overnight under vacuum to obtain **P(N_3-PPFPA).**

Synthesis of P1(N_3-OH)

50.0 mg (0.210 mmol) of **P(N_3-PPFPA)** with molecular weights of 7×10^4 and 2.3×10^5 g/mol, respectively, was added to small glass vials. The polymer was completely dissolved using 1 mL of THF. Subsequently, 13.1 mg (0.175 mmol) **IPA** was added. The reaction was allowed to proceed overnight at RT. The product was precipitated, washed twice with diethyl ether, and centrifuged at 1×10^4 r/min for 10 min to collect the product. The collected product was dissolved in water and freeze-dried to obtain **P1(N_3-OH)**.

Synthesis of P2(N_3-COOH)

50.0 mg (0.210 mmol) of **P(N_3-PPFPA)** with a molecular weight of 2.3×10^5 g/mol were added to small glass vials. The polymer was then completely dissolved using 500 μL). Subsequently, 13.1 mg (0.175 mmol) of **Gly** was added, followed by 500 μL of H_2O and 10 μL of DIPEA. The reaction was allowed to proceed overnight at RT. The product was precipitated, washed twice with isopropanol, and centrifuged at 1×10^4 r/min for 10 min to collect the product. The collected product was dissolved in water and freeze-dried to obtain **P2(N_3-COOH)**.

Synthesis of P3(N_3-$CONH_2$)

50.0 mg (0.210 mmol) of **P(N_3-PPFPA)** with a molecular weight of 2.3×10^5 g/mol was added to small glass vials and completely dissolved using 500 μL of THF. Subsequently, 15.4 mg (0.175 mmol) of **APA** was added, followed by 500 μL of DMSO and 20.0 μL of DIPEA. The reaction was allowed to proceed overnight at RT. The product was precipitated, washed twice with ethanol, and centrifuged at 1×10^4 r/min for 10 min to collect the product. The collected products were dissolved in water and freeze-dried to obtain **P3(N_3-$CONH_2$)**.

Synthesis of P4(N_3-$CONH_2$)

50.0 mg (0.210 mmol) of **P(N_3-PPFPA)** with a molecular weight of 2.3×10^5 g/mol was added to small glass vials and completely dissolved using 500 μL of THF. After allowing the mixture to react for 2 h, 6.13 mg (0.175 mmol) of **AS** was added, and the reaction was continued overnight at room temperature. The product was precipitated, washed twice in cold methanol, and centrifuged at 1×10^4 r/min for 10 min to collect the product. The collected product was dissolved in water and freeze-dried to obtain **P4(N_3-$CONH_2$)**.

Preparation of the Sequencing Chip

The sequencing chip was prepared using the method described by Salus BioMed Co. Ltd. The sequencing chip adopted a sandwich-like structure composed of a thin glass layer (about 0.150 mm), a double-sided polymethyl methacrylate (PMMA)

https://doi.org/10.1007/s10118-025-3413-8

tape with four channels (about 0.150 mm), and a thick glass layer (about 1.00 mm). The thin and thick glass slides were cleaned in piranha solution (a 3:1 mixture of concentrated sulfuric acid and hydrogen peroxide, highly corrosive, and handled with care) for 1 h to expose more silanol groups on the glass surface, followed by three rinses with deionized water. The cleaned thin glass was then modified with propargylsilane *via* a simplified chemical vapor deposition (CVD) method. The glass and prop-2-yn-1-yl(3-(triethoxysilyl)propyl)carbamate were placed in a vacuum oven and heated at 130 °C for 8 h. Finally, the thick glass and modified thin glass were bonded together using double-sided PMMA tape and a specialized mold. Next, the surface-modified polymer solution was injected into the lanes of the sequencing chip. The sequencing chip was sealed in vacuum at 60 °C for 1.5 h. Afterwards, the microfluidic lanes of the sequencing chip were washed with 3× SSC buffer using a dedicated microchannel cleaner from Salus BioMed Co., Ltd., yielding a sequencing chip available for subsequent use.

Fluorescence Intensity Test of Sequencing Chip

The four lanes of the prepared sequencing chip were filled with 3× SSC buffer, and then 30.0 μL of **DBCO-P7LG** (10.0 μmol) and 30.0 μL of **DBCO-P5LU** (10.0 μmol) were injected into the lanes, and heated in an oven at 38 °C overnight. The lanes were rinsed with 3× SSC buffer, followed by the injection of **P5-CY3** and **P7-CY3**, after which they were heated in an oven at 60 °C for 10 min. Then, the lanes were flushed with 3× SSC buffer twice and kept for standby. Fluorescent images were captured from left to right across the chip, and 240 images were captured to create a composite image of each lane. Fluorescence intensity values were calculated using ImageJ software. Lanes 1–3 were modified with the surface-modified polymer, whereas lane 4 was modified with the commercial control polymer.

SBS Reaction on the Sequencing Chip Utilizing Four Chemically Cleavable Fluorescent Nucleotides

Four lanes of the chip were washed with 3×SSC buffer. The instrument settings were configured by selecting the appropriate sequencing kit and chip type, with a typical "read length" of 150 base pairs. DNA sequencing was conducted over approximately 24 h. NGS technology, specifically the SBS method, was employed to determine the DNA sequence and generate a sequencing quality report. In the SBS process, four fluorescently labeled nucleotides with blocked 3'-OH ends were added.[48] Owing to blocking, each nucleotide could only pair with one complementary nucleotide at a time. The fluorescence was excited and identified using a laser. Finally, the fluorescent and blocking groups were removed to begin the next cycle. Based on this report, the sequencing performance of the experimental polymer-modified sequencing chips was evaluated. The sequences of the oligonucleotides used in this study were as follows: **DBCO-P7LG** bears DBCO-/iSp18//-iSp18/-TTTTTTTTTCAA/i8oxodG/-CAGAAGACGGCATACGAGAT (5'→3'), and **DBCO-P5LU** has the sequence DBCO-/iSp18//-iSp18/-TTTTTTTTTTT-AATGATACGGCGACCACCGAGA/ideoxyU/-CTACAC (5'→3'). P5C-CY3 and P7C-CY3 were labeled with Cy3 dye at their 5' ends, with sequences of TCGGTGGTCGCCGTATCATT and TCGTATGC-CGTCTTCTGCTTG (5'→3'), respectively. The four fluorescence-labeled nucleotides used for sequencing were A-atto532, T-atto640, G-atto680, and C-if700. Their specific structures are proprietary information that cannot be disclosed. All other sequencing-related materials were supplied by Salus BioMed Co. Ltd.

Characterization

A 400 MHz nuclear magnetic resonance (NMR) spectrometer (Bruker Co., Ltd.) was used for this test. To ensure the complete dissolution of the sample, the test sample was dissolved in $CDCl_3$ or D_2O and prepared into a solution with a concentration of 10.0 mg/mL. The chemical shift of the residual chloroform proton peak in $CDCl_3$ was accurately calibrated to 7.26 ppm, and similarly, the chemical shift of the residual acetonitrile proton peak in D_2O was calibrated to 4.80 ppm. Fourier-transform infrared (FTIR) spectroscopy (Bruker Co., Ltd.) was employed to analyze the functional groups of the polymers, with attenuated total reflection (ATR) as the sampling technique. After drying the sample, the powder (10.0 mg) was placed on the diamond crystal surface of the ATR accessory. Spectral acquisition was performed over a wavenumber range of 4000–400 cm^{-1} with 64 scans. The resulting infrared absorption spectrum underwent post-acquisition processing, including baseline correction, smoothing, and normalization, using the OMNIC software to enhance the quality and comparability of the data.

Size exclusion chromatography (SEC) was used to determine the molecular weight and the corresponding molecular weight dispersity ($Đ = M_w/M_n$) of **PPFPA** and the surface-modified polymers. The chromatographic apparatus used in this study consisted of an LC-100 high-pressure constant flow pump (Shanghai Wufeng Co., Ltd.), a Shodex RI201-II differential refractive index detector (Shimadzu Co., Ltd.), and a gel permeation column formed by the series connection of a Mono-GPC1000 column and KD-803 column. In the experiment, DMF containing tetrabutylammonium bromide (TBABr) at a concentration of 0.80 mg/mL was used as the mobile phase to prevent adsorption between the sample and column, and the sample concentration was set at 5.00 mg/mL. The flow rate of the high-pressure constant-flow pump was maintained at 1.00 mL/min, while the test temperature of the chromatographic column was maintained at 40 °C. A goniometer (Dataphysics Co., Ltd.) was used to detect the changes in the contact angle of the sequencing chip. Deionized water was used for water contact angle measurements. A water droplet of approximately 10.0 μL was dispensed each time and controlled automatically by a computer. After equilibration in air for approximately 5.00 s, a manual photograph was taken.

A gene sequencer from Salus Pro (Salus BioMed Co., Ltd.) was used to test the fluorescence intensity and performance of the sequencing chips. The lanes of the chip were washed with 3× SSC buffer. Fluorescent images were captured, with 240 images taken per lane to create a composite image of the entire lane. The ImageJ software was used to calculate the fluorescence intensity values from the captured images. The optical signals were converted into sequences of the target bases using the Basecall software. During sequencing, the control software automatically invoked the Basecall software for analysis and output the sequencing data to a designated location for secondary analysis. The typical sequencing read length was 150, corresponding to 150 cycles of single-end sequencing with a sequencing duration of approximately 24.0 h.

https://doi.org/10.1007/s10118-025-3413-8

RESULTS AND DISCUSSION

Synthesis of the PPFPA Platforms and Surface Modification Polymers

Commercial PAAm-based surface-modification polymers were prepared by the copolymerization of acrylamide and *N*-(5-(2-azidoacetamido)pentyl)acrylamide in a molar ratio of 5:1. The synthesis of azide-containing acrylamide monomers and the copolymerization of different acrylamide monomers are often complex and difficult to control in terms of molecular weight and monomer ratio. Thus, a systematic comparison between different surface-modified polymers with identical degrees of polymerization and monomer ratios would be difficult. To address this issue, we employed a post-polymerization approach to prepare a library of surface-modified polymers composed of two monomers in a molar ratio of 5:1 (Fig. 1a). In particular, a polymer platform of **PPFPA** was first synthesized with the desired molecular weight, followed by the transforming of 1/6 of the PFP units into azide-containing side groups (monomer-**1** in Fig. 1a). Finally, all the remaining PFP units were consumed by other amine species (monomer-**2** in Fig. 1a) to afford the final surface-modified polymers. In this manner, the degree of polymerization and monomer ratio of the surface-modified polymers could be well controlled.

The PFPA monomer was synthesized from pentafluorophenol and acrylic acid according to previously reported procedures with slight modifications[15]. The successful syntheses of PFPA and **PPFPA** were confirmed by NMR, FTIR, and SEC (see electronic supplementary information, ESI and Fig. 2). In the ^{1}H-NMR spectrum of PFPA, characteristic peaks at 6.72, 6.37 and 6.18 ppm correspond to the three protons on the acrylate group (see Fig. S1 in ESI). The ^{19}F-NMR spectrum of PFPA showed three distinct peaks at −153, −158, and −162 ppm, confirming the presence of fluorine atoms at different positions in the PFP group (see Fig. S1 in ESI). Subsequently, the normal radical polymerization of PFPA was conducted to prepare **PPFPA** with different molecular weights, which were controlled by tuning the monomer-to-initiator ratios. As shown in Figs. 2(A) and 2(B), the ^{1}H-NMR spectrum of **PPFPA** presents several broad peaks at 3.10, 2.48 and 2.10 ppm, while the ^{19}F-NMR spectrum of **PPFPA** exhibits three main peaks at the same positions as PFPA but with broader shapes, which confirms the successful synthesis of **PPFPA**. FTIR characterization of **PPFPA** was also performed, as shown in Fig. 2(C). The peaks at 1780, 1250, and 1500 cm^{-1} are attributed to the PFP groups in the polymer. The successful synthesis is also confirmed by SEC analysis, as shown in Fig. 2(D), with a clear trend of increasing molecular weight indicated by de-

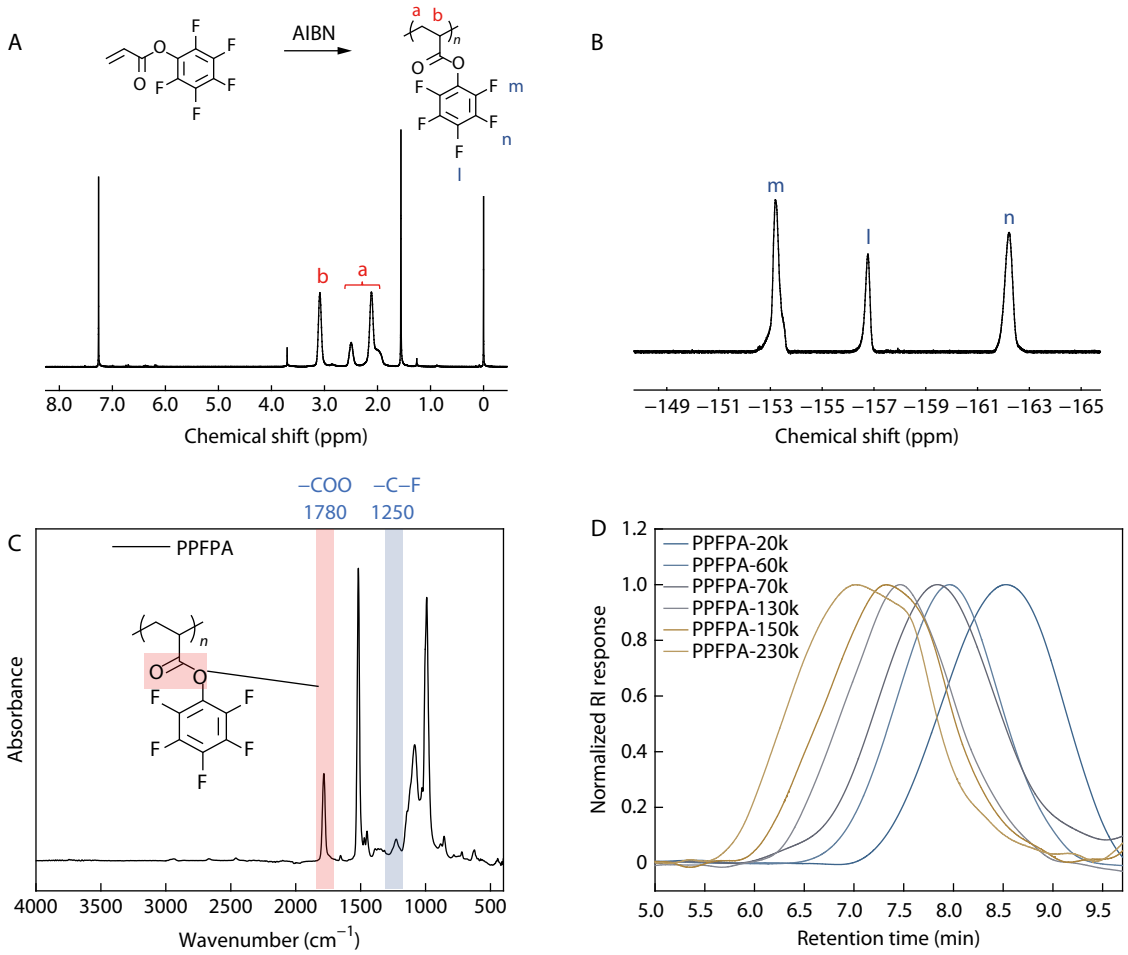

Fig. 2 Chemical characterization of the synthesized **PPFPA** platforms: (A) ^{1}H-NMR spectrum, (B)^{19}F-NMR spectrum, (C) FTIR spectrum and (D) SEC traces.

https://doi.org/10.1007/s10118-025-3413-8

Table 1 Chemical parameter summary of PPFPA platform polymers and surface modification polymers.

No.	Sample	M_w [a] (g/mol)	$Đ$ [b]	Monmer-**1**	Monmer-**2** [c]	Charge state [d]
1	**PPFPA**	0.70×10^5	2.0	/	/	0
2	**PPFPA**	2.30×10^5	2.1	/	/	0
3	**P(N_3-PFPA)**-C_5	0.70×10^5	2.0	NH_2-C_5-N_3	/	0
4	**P(N_3-PFPA)**-C_5	2.30×10^5	2.1	NH_2-C_5-N_3	/	0
5	**P(N_3-PFPA)**-EG_3	2.36×10^5	2.1	NH_2-EG_3-N_3	/	0
6	**P1(N_3-OH)**-C_5	0.43×10^5	/	NH_2-C_5-N_3	**IPA**	0
7	**P1(N_3-OH)**-C_5	1.42×10^5	/	NH_2-C_5-N_3	**IPA**	0
8	**P2(N_3-COOH)**-C_5	1.42×10^5	/	NH_2-C_5-N_3	**Gly**	–
9	**P3(N_3-$CONH_2$)**-C_5	1.53×10^5	/	NH_2-C_5-N_3	**APA**	+
10	**P4(N_3-$CONH_2$)**-C_5	0.96×10^5	/	NH_2-C_5-N_3	**AS**	+
11	**P1(N_3-OH)**-EG_3	1.47×10^5	/	NH_2-EG_3-N_3	**IPA**	0
12	**P2(N_3-COOH)**-EG_3	1.48×10^5	/	NH_2-EG_3-N_3	**Gly**	–
13	**P3(N_3-$CONH_2$)**-EG_3	1.58×10^5	/	NH_2-EG_3-N_3	**APA**	+
14	**P4(N_3-$CONH_2$)**-EG_3	1.01×10^5	/	NH_2-EG_3-N_3	**AS**	+

[a] The weight-average molecular weights were predicted based on the theoretical molecular weight of 2.3×10^5 g/mol of **PPFPA** modified with a 1:5 ratio of N_3 to hydrophilic molecules. [b] Molecular weight dispersity is represented by $Đ$. [c] Surface modification polymers were modified with isopropanolamine, glycine, 3-aminopropanamide, and ammonia solution, designated as **IPA**, **Gly**, **APA**, and **AS**, respectively. [d] The dPositive, negative, and neutral states are represented by +, – and 0, respectively.

creasing retention time from 8.51 min to 7.03 min, corresponding to **PPFPA** molecular weights from 2×10^4 g/mol to 2.3×10^5 g/mol, respectively. The SEC curves exhibited symmetric, monodisperse peaks, reflecting a moderate molecular weight dispersity ($Đ$) and uniform molecular weight distribution, which is critical for consistent material properties and reproducibility. The molecular information of all the synthesized polymers is summarized in Table 1.

A two-step post-polymerization treatment was then performed to transform the **PPFPA** platform polymers into the desired surface modification polymers for sequencing chips. One component provides azide groups (monomer-**1**) to specifically and efficiently immobilize **DBCO-P7LG** and **DBCO-P5LU** primers onto the surface. The other provides hydrophilic groups (monomer-**2**) to enhance the biocompatibility and hydrophilicity of the chip surface, preventing bubble formation when liquids are injected into the channels. According to previous studies and the commercial utilization of PAAm-based copolymers, a 1:5 ratio of azide to acrylamide is optimal for sequencing performance.[49] Thus, this study adopts a 1:5 ratio of monomer-**1** to monomer-**2** to prepare the surface-modified polymers. In the first step of the post-polymerization treatment, 1/6 of the PFP units on **PPFPA** were transformed into azide-containing side groups by either of two amine species: **NH_2-C_5-N_3** and **NH_2-EG_3-N_3.** The former possesses five carbon atoms and one amide bond between the amino and azide groups, whereas the latter has three repeating ethylene glycol (EG) units in the middle. The FTIR spectra, shown in Fig. 3(a), provide clear evidence of the successful modification of **PPFPA** with various functional groups *via* amidation. The introduction of the N_3 group is confirmed by the characteristic absorption peak at approximately 2100 cm^{-1}, attributed to the N_3 stretching vibration. Moreover, the ^{1}H-NMR spectrum Fig. 2(B) confirmed the successful amidation of monomer-**1**, showing a peak at 3.99 ppm.

In the second step, another four amine species with different charge states, **IPA**, **Gly**, **APA** and **AS,** were applied to react with the remaining PFP groups, affording the ultimate surface modification polymers. **P1(N_3-OH)** and **P2(N_3-COOH)** possess hydroxyl and carboxyl groups in monomer-**2**, which show neutral and negative charge states in aqueous solution.

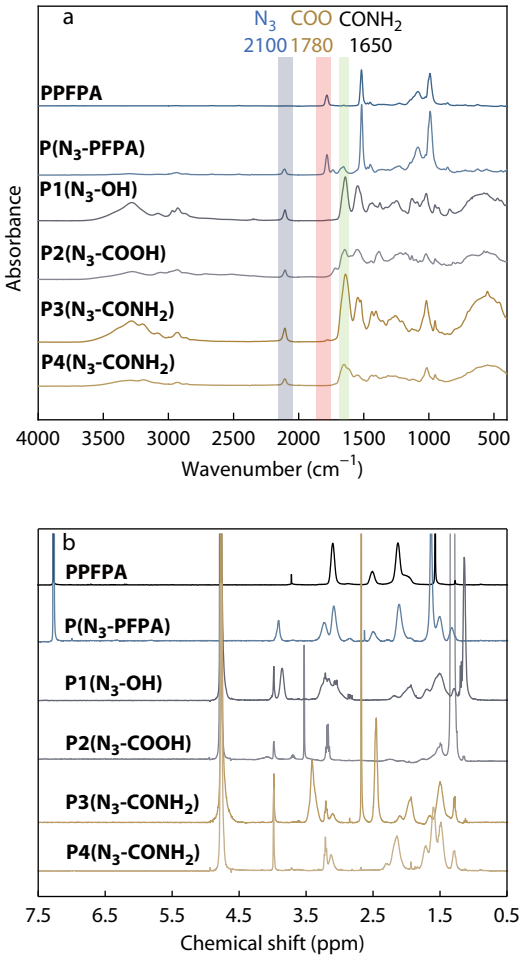

Fig. 3 (a) FTIR and (b) ^{1}H-NMR spectra of **PPFPA**-230k and corresponding surface modification polymers with **NH_2-C_5-N_3** as monomer-**1**, and **IPA**, **Gly**, **APA** or **AS** as monomer-**2**.

https://doi.org/10.1007/s10118-025-3413-8

The chemical difference lies in the fact that **P3(N_3-$CONH_2$)** has one more amide group than **P4(N_3-$CONH_2$)**. Notably, the commercial PAAm-based surface-modification polymer had the same chemical composition as **P4(N_3-$CONH_2$)**. As shown in Fig. 3(a), the disappearance of the peak at 1780 cm^{-1} in the FTIR spectra of all surface-modified polymers indicates that the PFP group was completely removed and transformed into monomer-**2**. The introduction of **IPA**, **Gly**, and **APA** was confirmed by the characteristic peaks in the ^{1}H-NMR spectrum at approximately 3.88, 3.55, and 3.44 ppm, respectively. By integrating the corresponding ^{1}H-NMR peaks, the ratios of anchoring sites to hydrophilic sites were determined to be approximately 1:5 for all surface-modified polymers.

DNA Primer Immobilization Efficacy Evaluation of Surface Modification Polymers

The synthesized polymers with versatile monomer-**1** and monomer-**2** combinations were used to modify the surface of the sequencing chips (see details in the experimental sections). Briefly, a pair of thin and thick glass slides was cleaned with piranha solution and then subjected to a CVD process using prop-2-yn-1-yl(3-(triethoxysilyl)propyl)carbamate to introduce an alkyne group on the surface. As shown in Fig. S2 (in ESI), the contact angles of the original thin and thick glass slides are 80.5° and 35.4°, respectively. After piranha cleaning, both contact angles were reduced to below 10°, confirming the effective removal of organic contaminants and the exposure of reactive silanol groups. The contact angle of the thin glass slide increased to 54.3°, indicating successful alkyne layer deposition. Then, the thin glass and thick glass were sealed into a four-lane microfluidic chip using PMMA double-sided adhesive tape.

A microfluidic control system was used to modify the surfaces of the synthesized polymers. The process began with the injection of surface-modified polymer solutions into the individual lanes of the sequencing chip. The chip was then heated to 60 °C for a duration of 1.5 h, allowing for the "click reaction" between the azide groups on the surface modification polymers and the alkyne groups on the chip surfaces. Following this, the microfluidic lanes of the sequencing chip were thoroughly flushed with 3× SSC buffer solution to remove unreacted polymers.

To compare the immobilization efficacy of the DNA primers, aqueous solutions of two common single stranded DNA (ssDNA) segments, **DBCO-P7LG** and **DBCO-P5LU**, were fluxed into the microfluidic lanes of the chip. As shown in Fig. 4, their immobilization on the chip surfaces was realized by the "click reaction" between the azide groups of the surface modification polymers and DBCO groups of the ssDNA segments. Then, solutions of the fluorophore-bearing complementary ssDNA, **P7-CY3** and **P5-CY3**, were fluxed into the chip lanes, which could be specifically paired with the readily immobilized **P7LG** and **P5LU,** respectively. **CY3** is a cyanine fluorescent dye that emits orange-red light (570 nm) when excited by a green light laser of 550 nm. Thus, the immobilization efficacy of the surface-modified polymers can be characterized by detecting the fluorescence intensity from paired **P5-CY3** and **P7-CY3**. Fluorescence intensity must reach a minimum limit for application in subsequent gene sequencing tests. Otherwise, the sequencing process was terminated if the fluorescence intensity was insufficient.

The results of the fluorescence intensity tests are shown in Fig 5. All the surface-modified polymers tested in Fig. 5(a) were prepared from the same batch of **PPFPA** with a molecular weight of 2.3×10^5 g/mol. Obviously, for polymer samples with the same type of monomer-**2**, those with **NH_2-C_5-N_3** as monomer-1 showed higher fluorescence intensity than those with **NH_2-EG_3-N_3** as monomer-**1**. **P1(N_3-OH)**-C_5 showed the largest difference in fluorescence intensity, which was 2.5 times higher than that of **P1(N_3-OH)**-EG_3. To explain this observation, it should be noted that the three ethylene glycol groups in **NH_2-EG_3-N_3** are hydrophilic, whereas the five ethy-

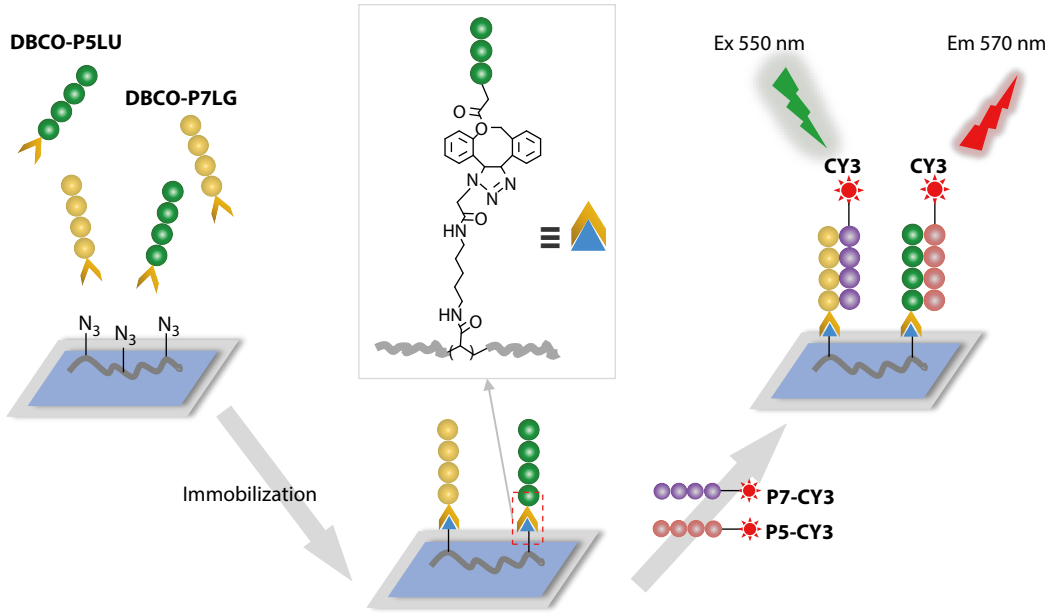

Fig. 4 Schematic representative showing the mechanism of evaluating the ssDNA primer immobilization efficacy by the fluorescence intensity tests.

https://doi.org/10.1007/s10118-025-3413-8

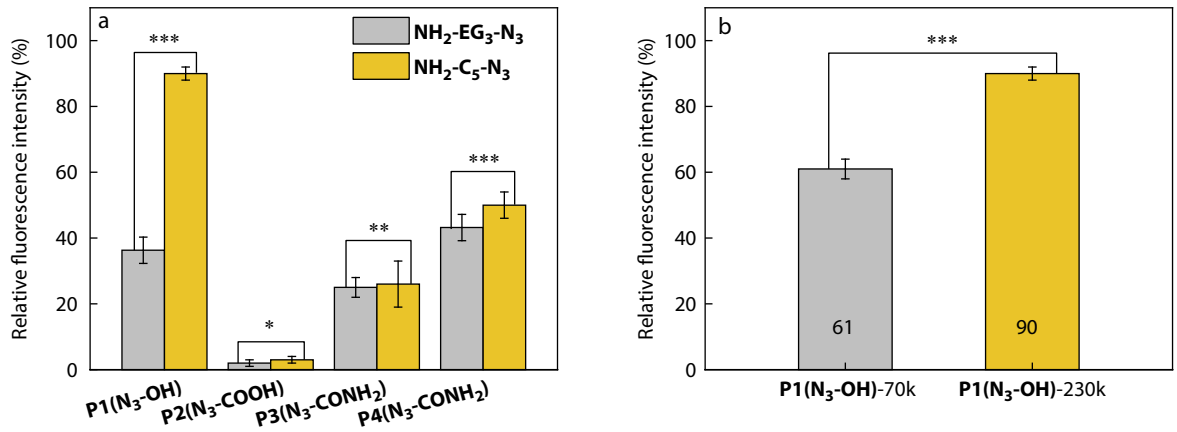

Fig. 5 Results of fluorescence intensity tests on sequencing chip lanes modified by polymers (a) derived from the same batch of PPFPA-230k but transformed with different combinations of monomer-**1** and monomer-**2**, and (b) of different molecular weights but the same composition of **NH_2-C_5-N_3** and Gly as monomer-**1** and monomer-**2**. P values were determined by one sample unpaired t-test. * $p < 0.05$, ** $p < 0.01$, *** $p < 0.001$

lene groups in **NH_2-C_5-N_3** are hydrophobic. Considering that monomer-**2** is hydrophilic, the chain conformation of polymers with both hydrophilic monomers would be similar to that of random coils, and the azide groups may not be efficiently exposed to react with the chip surface. However, if monomer-**1** is hydrophobic, the hydrophobic segments of the polymer chains tend to aggregate locally. Thus, the number density of azide groups is locally increased, leading to a high probability of reaction with the alkyne group on the chip surface. Once more polymers are attached, more ssDNA segments can be immobilized on the chip surface.

In addition, the polymer samples **P2(N_3-COOH)** with **Gly** as monomer-**2**, regardless of monomer-**1**, displayed the lowest fluorescence intensity, indicating the worst immobilization efficacy for the ssDNA segments. **P1(N_3-OH)**-C_5 achieved the highest fluorescence intensity, reaching 90% of the commercial polymer control value, whereas **P3(N_3-$CONH_2$)** and **P4(N_3-$CONH_2$)**, regardless of monomer-1, both attained 50% of the control value. This finding aligns with prior studies reporting that surface charge significantly influences interactions between biomolecules and cells, as evidenced by fungal detection[50] and extensive research on circulating tumor cells (CTCs).[51–54] In aqueous solutions, the negatively charged carboxyl groups induce strong electrostatic repulsion, impeding the approach of similarly negatively charged ssDNA segments. **P3(N_3-$CONH_2$)** and **P4(N_3-$CONH_2$)** both contain amide groups that are partially positive in water. This may cause electrostatic attraction of ssDNA to the surface, hindering the formation of covalent bonds between the azide and DBCO groups. Only **P1(N_3-OH)** has neutral hydroxyl groups, which can eliminate electrostatic effects and provide both hydrophilicity and biocompatibility for ssDNA immobilization.

It should be noted that **P4(N_3-$CONH_2$)** has the same chemical composition as the current commercial surface modification polymers, although it showed only half the fluorescence intensity of the commercial one. The molecular weight of the commercial polymer was much greater than that of **P4(N_3-$CONH_2$)**. To investigate the impact of molecular weight on immobilization efficacy, we synthesized low molecular weight **P1(N_3-OH)**-C_5-70k and compared its immobilization efficacy with **P1(N_3-OH)**-C_5-230k. As shown in Fig. 5(b), the high-molecular-weight polymer generally exhibited a higher fluorescence intensity than the low-molecular-weight polymer. This finding aligns with the results obtained for **P4(N_3-$CONH_2$)** and the commercial polymer. These elongated chains provided greater extension space and increased segment density, enabling enhanced surface spreading and the formation of additional contact points. Consequently, the fluorescence performance was improved. Based on the immobilization efficacy testing results, we eliminated **P2(N_3-COOH)** and **P3(N_3-$CONH_2$)** from the subsequent sequencing performance tests and only focused on the remaining two.

Real-time Gene Sequencing Performance Evaluation of P1(N_3-OH) and P4(N_3-$CONH_2$)

After sufficient ssDNA primers were immobilized onto the microfluidic chip surface, the aqueous solutions of the fragmented DNA library were fluxed through the flow cell, and bridge PCR was applied to amplify the DNA fragment library, as illustrated in Fig. 6(a). This process was aimed at large-scale DNA duplication on the chip lane surfaces, where many ssDNA primers had already been immobilized in the last procedure. Bridge PCR can generate dense clusters of duplicated DNA within a confined area, thereby providing abundant templates for subsequent sequencing-by-synthesis (Fig. 6b). During SBS, fluorescently labeled reversible terminator nucleotides were incorporated stepwise, with each cycle detecting the emitted fluorescence before cleaving the terminator for subsequent base additions. High-throughput SBS was achieved by the parallel sequencing of clustered DNA templates. As a result, the immobilization efficacy of ssDNA primers determined by the surface modification polymers would eventually affect the number density of clustered DNA templates on chip surfaces and make an impact on the sequencing performance.

In the last session, we screened all the surface modification polymers by fluorescence intensity testing and chose **P1(N_3-OH)**-C_5 and **P4(N_3-$CONH_2$)**-C_5 for the sequencing performance evaluation. These were synthesized from the same batch of **PPFPA**-230k. A real image of the four-lane sequencing chip is shown in Fig. 7(a). **P2(N_3-COOH)**-C_5, **P4(N_3-**

https://doi.org/10.1007/s10118-025-3413-8

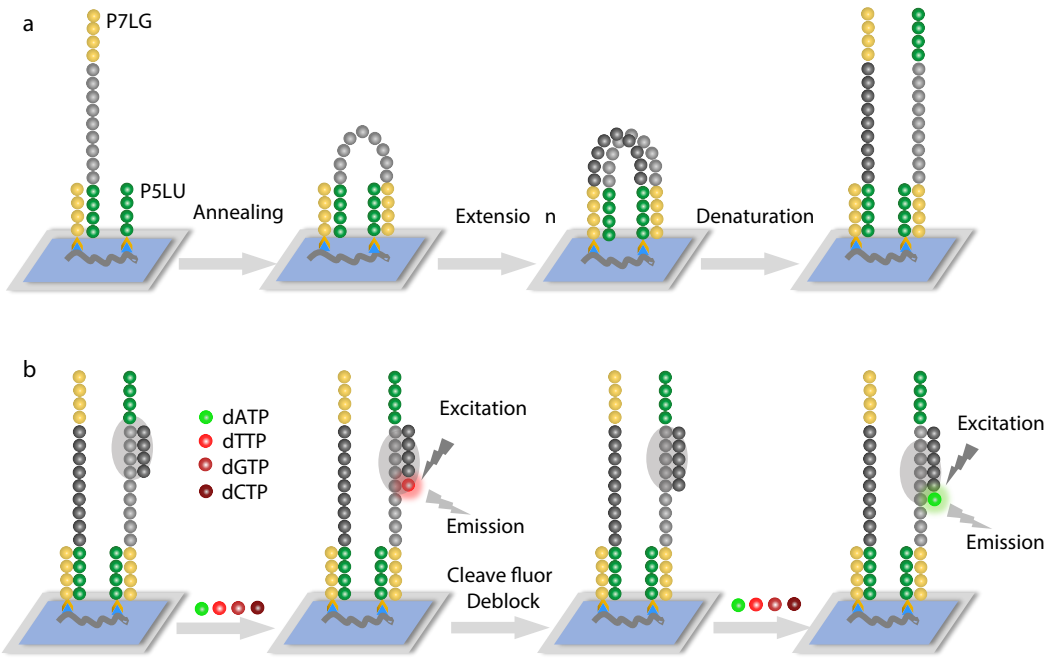

Fig. 6 Schematic representatives showing (a) the bridge PCR process and (b) the SBS process.

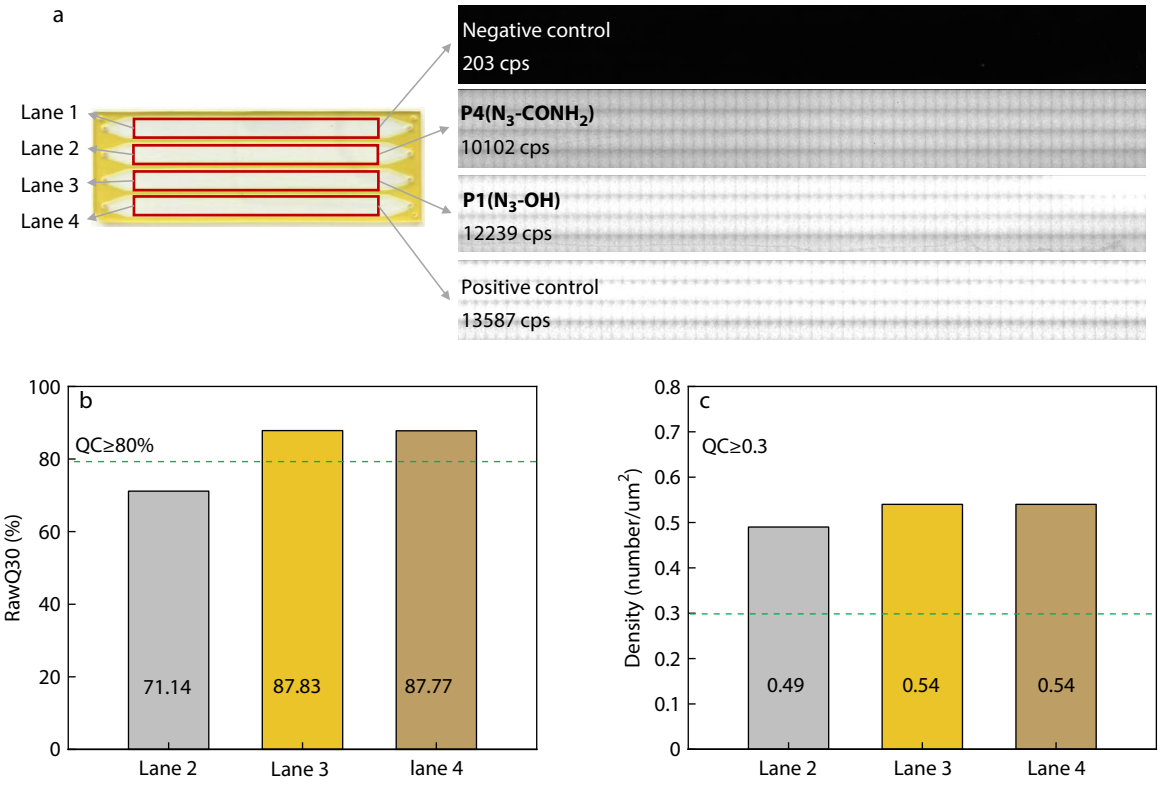

Fig. 7 (a) Real image and fluorescence test images of the four-lane sequencing chip modified by different polymers. The surface modification polymers, fluorescence brightness and intensity of each lane are displayed accordingly. (b) The RawQ30 values and (c) the grafting density values of Lanes 2–4 of the chip, reflecting their gene sequencing performance.

$CONH_2$)-C_5, **P1(N_3-OH)**-C_5 and commercial polymers were utilized for the surface modification of lanes 1 to 4, respectively. Notably, **P2(N_3-COOH)**-C_5 in lane 1 and the commercial polymer in lane 4 were used as negative and positive controls, respectively. Prior to bridge PCR, a fluorescence intensity test was performed to validate the immobilization of ssDNA primers. As shown in Fig. 7(a), lane 1 exhibited an extremely weak fluorescence intensity of 203 cps, while lane 3 demonstrated a significantly higher intensity of 12,239 cps, which was very close to that of the positive control lane 4.

https://doi.org/10.1007/s10118-025-3413-8

Bridge PCR of the fragmented DNA library was carried out in lanes 2, 3, and 4. Subsequently, the sequencing kit solutions, including polymerase and four fluorophore-modified nucleotides, were programmatically fluxed in lanes 2, 3, and 4 for the SBS process.

The sequencing performances of **P1(N_3-OH)**-C_5 and **P4(N_3-$CONH_2$)**-C_5 are summarized in Figs. 7(b) and 7(c), respectively. Here, RawQ30 was defined as the percentage of bases in raw sequencing reads that have a sequencing quality value exceeding 30, which corresponds to an error rate of less than 0.1%.[55] This metric is crucial for assessing the accuracy and reliability of sequencing data. Thus, a higher RawQ30 value indicates more accurate and reliable raw sequencing data. Sequencing results, as shown in Fig. 7(b), confirmed superior sequencing performance of **P1(N_3-OH)**-C_5, with RawQ30 values reaching 87.8%, exceeding the 80.0% quality control (QC) threshold. Moreover, the RawQ30 value of **P1(N_3-OH)**-C_5 in lane 1 slightly exceeded that of the commercial polymer in lane 4, whereas that of **P4(N_3-$CONH_2$)**-C_5 in lane 2 did not pass the QC line. Although **P4(N_3-$CONH_2$)**-C_5 has the same chemical composition as the commercial polymer, their differences in SBS performance were mainly due to the molecular weight impact, which was in accordance with the above fluorescence intensity tests.

Another crucial metric is the DNA cluster density. It represents the number of DNA clusters generated during SBS per unit area on the chip surface. Its value must not be lower than the 0.3 μm^{-2} QC threshold. Otherwise, insufficient density can cause low fluorescence intensity, making it difficult for the detector to recognize signals and leading to sequencing errors. As shown in Fig. 7(c), the DNA cluster density of **P1(N_3-OH)**-C_5 group reached 0.540 μm^{-2}, surpassing the QC standard of 0.300 μm^{-2} the **P4(N3-$CONH_2$)**-C_5 group. These findings demonstrate that **P1(N_3-OH)**-C_5 meets or exceeds key performance indices for sequencing applications. Sequencing data demonstrated that **PPFPA** serves as a versatile polymer platform compatible with NGS techniques.

CONCLUSIONS

In conclusion, this study successfully established an amine-reactive **PPFPA** platform for the high-performance surface modification of sequencing chips. Through post-polymerization functionalization, the platform was tailored with specific azide groups for efficient covalent immobilization of DBCO-modified DNA primers *via* click chemistry, along with diverse hydrophilic moieties to enhance surface biocompatibility and hydrophilicity. Systematic optimization revealed that hydrophobic azide carriers (**NH_2-C_5-N_3**) coupled with neutral hydroxyl groups (**IPA**) yielded the highest DNA immobilization efficacy. Furthermore, higher-molecular-weight polymers demonstrated significantly improved performance. The optimized **PPFPA**-based polymer **P1(N_3-OH)**-C_5 achieved exceptional sequencing metrics: a RawQ30 value of 87.8%, exceeding the quality control standard of 80%, and a high polymer surface density of 0.540 μm^{-2}, surpassing the QC threshold of 0.300 μm^{-2}. These results not only meet the QC standards, but are also comparable to the performance of current commercial polyacrylamide-based polymers that have been optimized for decades, highlighting the **PPFPA** platform's superior capability of the **PPFPA** platform in enabling sensitive and reliable NGS applications.

Conflict of Interests

The authors declare no interest conflict.

Electronic Supplementary Information

Electronic supplementary information (ESI) is available free of charge in the online version of this article at http://doi.org/10.1007/s10118-025-3413-8.

Data Availability Statement

The paper-related data are available from the corresponding author (liuh@dhu.edu.cn) upon reasonable request.

ACKNOWLEDGMENTS

This work was financially supported by the Science and Technology Commission of Shanghai Municipality (No. 24ZR1401400). The authors would like to express their sincere gratitude to Shenzhen Salus BioMed Company for their strong support in this study. We are grateful for the generosity of the company in providing the sequencing facilities and reagents.

REFERENCES

1 Goldenberg, A. J.; Dodson, D. S.; Davis, M. M.; Tarini, B. A. Parents' interest in whole-genome sequencing of newborns. *Genet. Med.* **2014**, *16*, 78–84.
2 Ziegler, A.; Koval-Burt, C.; Kay, D. M.; Suchy, S. F.; Begtrup, A.; Langley, K. G.; Hernan, R.; Amendola, L. M.; Boyd, B. M.; Bradley, J.; Brandt, T. Expanded newborn screening using genome sequencing for early actionable conditions. *JAMA* **2025**, *333*, 232–240.
3 Hilt, E. E.; Ferrieri, P. Next generation and other sequencing technologies in diagnostic microbiology and infectious diseases. *Genes* **2022**, *13*, 1566.
4 Lefterova, M. I.; Suarez, C. J.; Banaei, N.; Pinsky, B. A. Next-generation sequencing for infectious disease diagnosis and management: a report of the association for molecular pathology. *J. Mol. Diagn.* **2015**, *17*, 623–634.
5 Ginsburg, G. S.; Willard, H. F. Genomic and personalized medicine: foundations and applications. *Transl. Res.* **2009**, *154*, 277–287.
6 Pasche, B.; Absher, D. Whole-genome sequencing: a step closer to personalized medicine. *JAMA* **2011**, *305*, 1596–1597.
7 Katsanis, S. H. Molecular genetic testing and the future of clinical genomics. *Nat. Rev. Genet.* **2013**, *14*, 415–426.
8 Sanger, F.; Nicklen, S.; Coulson, A. R. DNA sequencing with chain-terminating inhibitors. *Proc. Natl. Acad. Sci.* **1977**, *74*, 5463–5467.
9 Gonzalez, F. S.; Ungar, W. J.; Buchanan, J.; Christodoulou, J.; Stark, Z.; Goranitis, I. Microcosting genomics: challenges and opportunities. *Genet. Med.* **2025**, *27*, 101310.
10 Lambert, C. L.; van Mierlo, G.; Bues, J. J.; Guillaume-Gentil, O. J.; Deplancke, B. The evolution of DNA sequencing with microfluidics. *Nat. Rev. Genet.* **2025**, *26*, 1–2.
11 Recharla, M.; Nuka, S. T.; Chakilam, C.; Chava, K.; Suura, S. R. Next-generation technologies for early disease detection and

treatment: harnessing intelligent systems and genetic innovations for improved patient outcomes. *J. Reattach. Ther. Dev. Divers.* **2023**, *6*, 1921–1937.
12 Hu, Y.; Jiang, L.; Sun, X.; Wu, J.; Ma, L.; Zhou, Y.; Lin, K.; Luo, Y.; Cui, C. Risk assessment of antibiotic resistance genes in the drinking water system. *Sci. Total Environ.* **2021**, *800*, 149650.
13 Ni Raghallaigh, H.; Eeles, R. Genetic predisposition to prostate cancer: an update. *Fam. Cancer* **2022**, *21*, 101–114.
14 Uitto, J.; Saeidian, A. H.; Youssefian, L.; Vahidnezhad, H. Interpretation of genomic sequence variants in heritable skin diseases: A primer for clinicians. *J. Am. Acad. Dermatol.* **2023**, *89*, 569–576.
15 Crossley, B. M.; Bai, J.; Glaser, A.; Maes, R.; Porter, E.; Killian, M. L.; Clement, T.; Toohey-Kurth, K. Guidelines for Sanger sequencing and molecular assay monitoring. *J. Vet. Diagn. Investig.* **2020**, *32*, 767–775.
16 Kircher, M.; Kelso, J. High-throughput DNA sequencing–concepts and limitations. *Bioessays* **2010**, *32*, 524–536.
17 Totomoch-Serra, A.; Marquez, M. F.; Cervantes-Barragán, D. E. Sanger sequencing as a first-line approach for molecular diagnosis of Andersen-Tawil syndrome. *F1000Research* **2017**, *6*, 1016.
18 Jørgensen, T. S.; Blin, K.; Kuntke, F.; Salling, H. K.; Michaelsen, T. Y.; Albertsen, M.; Larsen, H. A rapid, cost efficient and simple method to identify current SARS-CoV-2 variants of concern by Sanger sequencing part of the spike protein gene. *medRxiv* **2021**, DOI: 10.1101/2021.03.27.21252266.
19 Anggraini, D.; Ota, N.; Shen, Y.; Tang, T.; Tanaka, Y.; Hosokawa, Y.; Li, M.; Yalikun, Y. Recent advances in microfluidic devices for single-cell cultivation: methods and applications. *Lab Chip.* **2022**, *22*, 1438–1468.
20 Shendure, J.; Ji, H. Next-generation DNA sequencing. *Nat. Biotechnol.* **2008**, *26*, 1135–1145.
21 Lincoln, S. E.; Hambuch, T.; Zook, J. M.; Bristow, S. L.; Hatchell, K.; Truty, R.; Kennemer, M.; Shirts, B. H.; Fellowes, A.; Chowdhury, S.; Klee, E. W. One in seven pathogenic variants can be challenging to detect by NGS: an analysis of 450,000 patients with implications for clinical sensitivity and genetic test implementation. *Genet. Med.* **2021**, *23*, 1673–1680.
22 Fusaro, M.; Rosain, J.; Grandin, V.; Lambert, N.; Hanein, S.; Fourrage, C.; Renaud, N.; Gil, M.; Chevalier, S.; Abou Chahla, W.; Bader-Meunier, B. Improving the diagnostic efficiency of primary immunodeficiencies with targeted next-generation sequencing. *J. Allergy Clin. Immunol.* **2021**, *147*, 734–737.
23 Noble, D. DNA sequencing on a chip. *Anal. Chem.* **1995**, *67*, 201A–204A.
24 Garrido-Cardenas, J. A.; Garcia-Maroto, F.; Alvarez-Bermejo, J. A.; Manzano-Agugliaro, F. DNA sequencing sensors: an overview. *Sensors* **2017**, *17*, 588.
25 Uhlen, M.; Quake, S. R. Sequential sequencing by synthesis and the next-generation sequencing revolution. *Trends Biotechnol.* **2023**, *41*, 1565–1572.
26 Zheng, Z.; Liebers, M.; Zhelyazkova, B.; Cao, Y.; Panditi, D.; Lynch, K. D.; Chen, J.; Robinson, H. E.; Shim, H. S.; Chmielecki, J.; Pao, W. Anchored multiplex PCR for targeted next-generation sequencing. *Nat. Med.* **2014**, *20*, 1479–1484.
27 Jurak, M.; Wiącek, A. E.; Ładniak, A.; Przykaza, K.; Szafran, K. What affects the biocompatibility of polymers. *Adv. Colloid Interface Sci.* **2021**, *294*, 102451.
28 Kim, H.; Jebrail, M. J.; Sinha, A.; Bent, Z. W.; Solberg, O. D.; Williams, K. P.; Langevin, S. A.; Renzi, R. F.; Van de Vreugde, J. L.; Meagher, R. J.; Schoeniger, J. S. A microfluidic DNA library preparation platform for next-generation sequencing. *PLoS One.* **2013**, *8*, e68988.
29 LeSavage, B. L.; Suhar, R. A.; Broguiere, N.; Lutolf, M. P.; Heilshorn, S. C. Next-generation cancer organoids. *Nat. Mater.* **2022**, *21*, 143–159.
30 Rashid, J. I. A.; Yusof, N. A. The strategies of DNA immobilization and hybridization detection mechanism in the construction of electrochemical DNA sensor: a review. *Sens. Bio-Sensing Res.* **2017**, *16*, 19–31.
31 Meng, X.; O'Hare, D.; Ladame, S. Surface immobilization strategies for the development of electrochemical nucleic acid sensors. *Biosens. Bioelectron.* **2023**, *237*, 115440.
32 Willams, J.; Anderson, J. **2005**, U.S. Pat., 20050266456
33 Adessi, C.; Kawashima, E.; Mayer, P.; Mermod, J. J.; Turcatti, G. **2000**, PCT Pat., 2000018957
34 Ramanathan, A.; Huff, E. J.; Lamers, C. C.; Potamousis, K. D.; Forrest, D. K.; Schwartz, D. C. An integrative approach for the optical sequencing of single DNA molecules. *Anal. Biochem.* **2004**, *330*, 227–241.
35 Wu, C.; Quesada, M. A.; Schneider, D. K.; Farinato, R.; Studier, F. W.; Chu, B. Polyacrylamide solutions for DNA sequencing by capillary electrophoresis: Mesh sizes, separation and dispersion. *Electrophoresis* **1996**, *17*, 1103–1109.
36 Müller, S.; Raulefs, S.; Bruns, P.; Afonso-Grunz, F.; Plötner, A.; Thermann, R.; Jäger, C.; Schlitter, A. M.; Kong, B.; Regel, I.; Roth, W. K. Next-generation sequencing reveals novel differentially regulated mRNAs, lncRNAs, miRNAs, sdRNAs and a piRNA in pancreatic cancer. *Mol. Cancer* **2015**, *14*, 1–18.
37 Ku, J.; Kim, S.; Park, J.; Kim, T. S.; Kharbash, R.; Shin, E. C.; Char, K.; Kim, Y.; Li, S. Reactive polymer targeting dsRNA as Universal virus detection platform with enhanced sensitivity. *Biomacromolecules* **2020**, *21*, 2440–2454.
38 Wu, J. S.; Hou, W.M.; Liu, Z. J.; Shi, Y.; Chen, Y.M. Mainchain semifluorinated polymers with ultra high molecular weight via reaction-enhanced reactivity of intermediate (RERI) mechanism. *Chinese J. Polym. Sci.* **2023**, *41*, 760–767.
39 Li, C.; Zhang, J. N.; Jin, J.; Jiang, W. The effect of topologies and refilling short-chain PEG on protein adsorption. *Chinese J. Polym. Sci.* **2023**, *41*, 1879–1888.
40 Wu, Y. C.; Huang, G. T.; Lian, M. Y.; Liang, R.; Deng, H. L.; Gan, F.; Zhang, Y. F.; Yi, N. B.; Tian, L.Y.; Ma, C. P.; Wei, Y. Modified triphenylmethane-based polyimides with improved optical, dielectric and solubility properties *via* post-polymerization modification. *Chinese J. Polym. Sci.* **2023**, *41*, 1609–1616.
41 McRae, S.; Chen, X.; Kratz, K.; Samanta, D.; Henchey, E.; Schneider, S.; Emrick, T. Pentafluorophenyl ester-functionalized phosphorylcholine polymers: preparation of linear, two-arm, and grafted polymer-protein conjugates. *Biomacromolecules* **2012**, *13*, 2099–2109.
42 Gibson, M. I.; Fröhlich, E.; Klok, H. A. Postpolymerization modification of poly(pentafluorophenyl methacrylate): synthesis of a diverse water-soluble polymer library. *J. Polym. Sci. Part A: Polym. Chem.* **2009**, *47*, 4332–4345.
43 Kim, S.; Ku, J.; Park, J.; Kharbash, R.; Li, S. Preparation of poly(pentafluorophenyl acrylate) functionalized SiO_2 beads for protein purification. *J. Vis. Exp.* **2018**, *141*, e58843.
44 Son, H.; Ku, J.; Kim, Y.; Li, S.; Char, K. Amine-reactive poly(pentafluorophenyl acrylate) brush platforms for cleaner protein purification. *Biomacromolecules* **2018**, *19*, 951–961.
45 Yue, K.; Liu, C.; Guo, K.; Yu, X.; Huang, M.; Li, Y.; Wesdemiotis, C.; Cheng, S. Z. D.; Zhang, W. B. Sequential "click" approach to polyhedral oligomeric silsesquioxane-based shape amphiphiles. *Macromolecules* **2012**, *45*, 8126–8134.
46 Noree, S.; Tangpasuthadol, V.; Kiatkamjornwong, S.; Hoven, V. P. Cascade post-polymerization modification of single pentafluorophenyl ester-bearing homopolymer as a facile route to redox-responsive nanogels. *J. Colloid Interface Sci.* **2017**, *501*, 94–102.

47 McKenna, M.; Soberon, F.; Ricco, A. J.; Daniels, S.; Kelleher, S. M. Click chemistry as an immobilization method to improve oligonucleotide hybridization efficiency for nucleic acid assays. *Sens. Actuators B Chem.* **2016**, *236*, 286–293.
48 Ju, J.; Kim, D. H.; Bi, L.; Meng, Q.; Bai, X.; Li, Z.; Li, X.; Marma, M. S.; Shi, S.; Wu, J.; Edwards, J. R. Four-color DNA sequencing by synthesis using cleavable fluorescent nucleotide reversible terminators. *Proc. Natl. Acad. Sci.* **2006**, *103*, 19635–19640.
49 George, W. N.; Brown, A. A.; Bratton, D.; Ren, H.; Smith, R. C. **2019,** U.S. Pat., 20190233890
50 Tian, W.; Li, F.; Wu, S.; Li, G.; Fan, L.; Qu, X.; Jia, X.; Wang, Y. Efficient capture and T2 magnetic resonance assay of candida albicans with inorganic nanoparticles: role of nanoparticle surface charge and fungal cell wall. *ACS Biomater. Sci. Eng.* **2019**, *5*, 3270–3278.
51 Wu, S.; Wang, P.; Qin, J.; Pei, Y.; Wang, Y. GSH-depleted nanozymes with dual-radicals enzyme activities for tumor synergic therapy. *Adv. Funct. Mater.* **2021**, *31*, 2102160.
52 Myung, J. H.; Launiere, C. A.; Eddington, D. T.; Hong, S. Enhanced tumor cell isolation by a biomimetic combination of E-selectin and anti-EpCAM: implications for the effective separation of circulating tumor cells (CTCs). *Langmuir* **2010**, *26*, 8589–8596.
53 Li, C.; Li, R.; Wu, X.; Zuo, Y.; Xiong, G.; Huang, M.; Sun, Y.; Liao, R.; Xiao, Y.; Hu, L.; Gao, C. Capture of heterogeneous circulating tumor cells in colorectal cancer patients on an immunomagnetic and anti-nonspecific adsorption platform. *Anal. Chem.* **2022**, *94*, 15240–15249.
54 Wu, S.; Gu, L.; Qin, J.; Zhang, L.; Sun, F.; Liu, Z.; Wang, Y.; Shi, D. Rapid label-free isolation of circulating tumor cells from patients' peripheral blood using electrically charged Fe_3O_4 nanoparticles. *ACS Appl. Mater. Interfaces* **2020**, *12*, 4193–4203.
55 Wu, W.; Xu, W. J.; Liu, J. B.; Sun, J.; Huang, Y. M.; Lu, Z. B. Exome sequencing identifies predisposing and fusion gene in ganglioneuroma, ganglioneuroblastoma and neuroblastoma. *Math Biosci. Eng.* **2019**, *16*, 7217–7229.

https://doi.org/10.1007/s10118-025-3413-8